ANTIOXIDANTS & REDOX SIGNALING
Volume 11, Number 6, 2009

DOI: 10.1089/ars.2009.2392

Forum Original Research Communication

Cross-Talk Between Mitochondria and NADPH Oxidase: Effects of Mild Mitochondrial Dysfunction on Angiotensin II-Mediated Increase in Nox Isoform Expression and Activity in Vascular Smooth Muscle Cells

João Wosniak Jr.,[1] Célio X. C. Santos,[1] Alicia J. Kowaltowski,[2] and Francisco R. M. Laurindo[1]

Abstract

Mitochondria and NADPH oxidase activation are concomitantly involved in pathogenesis of many vascular diseases. However, possible cross-talk between those ROS-generating systems is unclear. We induced mild mitochondrial dysfunction due to mitochondrial DNA damage after 24 h incubation of rabbit aortic smooth muscle (VSMC) with 250 ng/mL ethidium bromide (EtBr). VSMC remained viable and had 29% less oxygen consumption, 16% greater baseline hydrogen peroxide, and unchanged glutathione levels. Serum-stimulated proliferation was unaltered at 24 h. Although PCR amplification of several mtDNA sequences was preserved, D-Loop mtDNA region showed distinct amplification of shorter products after EtBr. Such evidence for DNA damage was further enhanced after angiotensin-II (AngII) incubation. Remarkably, the normally observed increase in VSMC membrane fraction NADPH oxidase activity after AngII was completely abrogated after EtBr, together with failure to upregulate Nox1 mRNA expression. Conversely, basal Nox4 mRNA expression increased 1.6-fold, while being unresponsive to AngII. Similar loss in AngII redox response occurred after 24 h antimycin-A incubation. Enhanced Nox4 expression was unassociated with endoplasmic reticulum stress markers. Protein disulfide isomerase, an NADPH oxidase regulator, exhibited increased expression and inverted pattern of migration to membrane fraction after EtBr. These results unravel functionally relevant cross-talk between mitochondria and NADPH oxidase, which markedly affects redox responses to AngII. *Antioxid Redox Signal* 11, 1265–1278.

Introduction

Enzymatic production of reactive oxygen species (ROS) is a major aspect of cell signaling in physiological or pathological conditions. Nox family NADPH oxidases are membrane-bound enzyme complexes representing the major source of signaling ROS (9, 26) in eukaryotic cells, particularly multicellular organisms (25). Nox(es) are involved in several vascular diseases, including atherosclerosis, hypertension, and diabetes mellitus (26), as well as aging (24). However, aging (8, 14) as well as most such diseases (20, 33) also importantly involve mitochondrial dysfunction, leading to derangements in energy metabolism, calcium homeostasis, and particularly ROS generation. Indeed, activities of electron transport chain (49) and other enzymes (44) within mitochondria are in quantitative terms the main cellular ROS source, while being a prototype of advantageous compartmentalization of redox processes. Mitochondrial superoxide is generated in quantal stochastic bursts (53) and may be mainly contained or scavenged within the organelle (41). Meanwhile, its by-product hydrogen peroxide diffuses outside mitochondria and regulates redox balance at a cellular level (15, 51), leading to large-scale switches in signaling programs controlling cell metabolism, differentiation, senescence, and apoptosis (15). In contrast, Nox(es) catalyze a low-output production of ROS in a way quite often highly

[1]Vascular Biology Laboratory, Heart Institute (InCor), University of São Paulo School of Medicine, São Paulo, Brazil.
[2]Departamento de Bioquimica, Instituto de Quimica da Universidade de São Paulo, São Paulo, Brazil.

compartmentalized and triggered by specific agonists (35, 46, 50). This implies that Noxes may likely integrate with mitochondria in order to achieve signaling coherence at cellular and supracellular levels. However, such cross-talk between mitochondria and NADPH oxidase is yet unclear and poorly explored. This knowledge would be particularly important in models of mild mitochondrial dysfunction, which has the potential to become sustained over time. In one direction, it has been suggested that NADPH oxidase might trigger ROS from mitochondria, in a way perhaps analogous to the known ROS-mediated ROS release (59). In addition, increased ROS generation by mitochondria isolated from endothelial cells exposed to AngII can be inhibited by cell incubation with siRNA against p22phox (11). Conversely, there is evidence that after serum withdrawal in HEK293 cells, mitochondrial-derived ROS activate, via PI3-kinase/Rac1, sustained ROS production from Nox1 (28). Mitochondrial dysfunction may result from several causes, including mutations in mitochondrial DNA (mtDNA) (1, 3, 6, 22, 23, 37, 49, 54) that lead to cumulative damage to electron transport chain components that further amplify dysfunction, as suggested by the occurrence of mtDNA mutations in many disease states. Experimental incubation of a variety of cell types with DNA-intercalating compounds such as ethidium bromide (EtBr) promotes preferential damage of mitochondrial rather than nuclear DNA (1, 22, 23, 57). If used on a sustained basis, EtBr incubation can generate cells that are viable (the so-called ρ^- or ρ^0 cells), but partially or completely depleted of mtDNA and thus devoid of mitochondrial electron transport chain components (22, 23). In the present study, we used an analogous but short-term EtBr incubation in VSMC to generate a model of what we defined as mild mitochondrial dysfunction (*i.e.,* neither rapidly lethal nor promoting profound redox derangements). In this model, we assessed the upstream role of mitochondria in NADPH oxidase-dependent responses to AngII. Our results indicate that mild mitochondrial dysfunction strongly affects activity and expression of Nox isoforms, providing novel direct evidence of a functionally relevant cross-talk between those major ROS-generating systems.

Methods

Reagents

Dihydroethidium, Amplex Red®, and PCR reagents were from Invitrogen (Carlsbad, CA). Culture medium, penicillin/streptomycin, fetal bovine serum, trypsin, and pancreatin were from Gibco BRL-Life Technologies (Grand Island, MD). All other chemicals, including ethidium bromide, were from Sigma (St. Louis, MO). All solutions were prepared with distilled water further purified in a Millipore Milli-Q system, in some experiments treated with Chelex-100 before use.

Generation and culture of pseudo-ρ^0 cells

Rabbit aortic smooth muscle cells (VSMC) from a previously established selection-immortalized line (5) were grown in F-12 medium supplemented with 10% FBS at 37°C in humidified atmosphere of 5% CO_2 and 95% air. Pseudo-ρ^0 VSMC were generated when cells grown at 80–95% confluence in 100 mm dishes were exposed to 250 ng/mL ethidium bromide (EtBr) for 24 h (up to 72 h in specified experiments), while kept in F-12 medium supplemented with 10% FBS and uridine (50 μg/mL) (22). The choice of EtBr concentration was based on validation experiments in which an initial number of 10^4 cells/mL was seeded in the absence of EtBr or its presence in concentrations of 25–10^4 ng/mL, and cell number was assessed 5 days later. The EC_{50} for EtBr (concerning a decrease in cell number) was 845 ng/mL, while 250 ng/mL induced 24% decrease (*vs.* control) in cell number after 5 days. No evidence of cell death (detachment and Trypan Blue assays) was found up to 500 ng/mL EtBr, while increased cell death occurred at higher concentrations. Thus, we selected the concentration of 250 ng/mL for 24 h as the standard for subsequent studies, since under these conditions there was no change in cell number and viability (see also Results section). Most experiments with ρ^0 cells in the literature involve supplementation with pyruvate (22). Since the concentration of pyruvate in F-12 medium is 2 m*M*, well within the range of final concentrations achieved in such experiments, additional pyruvate supplementation was not required. Similarly, mtDNA depletion usually requires supplementation of uridine in order to compensate for the fact that its synthetic enzyme dihydroorotate dehydrogenase is located at inner mitochondrial membrane and is impaired by EtBr (23). In our VSMC experiments, uridine supplementation alone did not alter cell number or NADPH oxidase activity.

mtDNA damage assessment by PCR amplification of the D-loop repetitive sequence region

Depletion of mtDNA after long-term EtBr exposure in ρ^0 cells is usually assessed by failure of PCR-triggered amplification of segments coding for specific enzymes (7, 22, 38, 39). We confirmed in preliminary experiments that even a 24 h exposure to EtBr leads to a failure to amplify the DNA region covering NADH dehydrogenase I through ATP 6 synthase in HEK293 cells (data not shown, corresponding to primer *a* from the rabbit sequence in Fig. 1A). In this case, such a failure of PCR amplification probably does not reflect complete mtDNA depletion, but rather damage to tertiary mtDNA structure, breakdowns, or deletion(s) (37, 57, 58), all of which can render primers out of frame and/or disrupt PCR amplification. In addition, EtBr can disrupt synthesis of mitochondria-associated RNA (57). However, in our VSMC, we consistently failed to detect any lack of PCR amplification of a number of short- or long-range primer combinations covering the entire coding and intergenic regions of rabbit mtDNA (Fig. 1A). Such reactions were carried out with 100–200 ng DNA and Regular, Platinum, or High-fidelity Taq or Pfx polymerase (Invitrogen) and cycle temperatures recommended by the manufacturer. While this method is likely not sensitive to exclude the occurrence of mtDNA damage, this finding is in line with the mild nature of induced mitochondrial dysfunction. Further investigation was therefore performed in the noncoding mtDNA D-loop region, known to regulate mtDNA replication during mitochondrial biogenesis (13, 19). The triple-strand D-loop sequence is highly variable among species and is a preferential site for point mutations, insertion/deletions, or rearrangements, which furthermore serve as marker for mtDNA alterations in pathologic conditions (4). We thus designed PCR primers covering the D-loop second region of repetitive sequences (from bases 16610–17221) (Fig. 1B). Because of the repetitive sequences, several amplification products were predicted, with the following bp

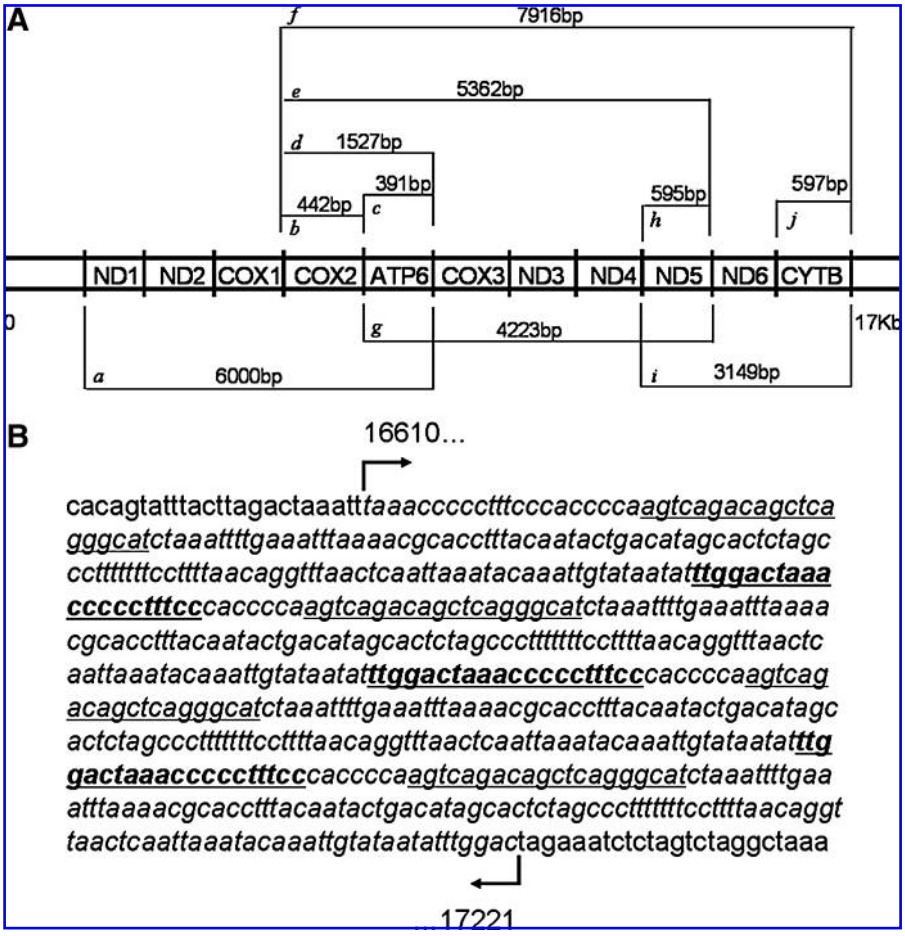

FIG. 1. Identification of mtDNA damage. (**A**) Scheme depicting the several primers used to investigate mutations in the coding region of rabbit mitochondrial DNA. The design of short- or long-range primers covered essentially all the coding region. (**B**) Published sequence of D-Loop second repetitive region (NCBI accession number NC_001913) spanning bases 16610 to 17221 (*italic characters*). Regions binding to right ("reverse") primer are underlined and regions binding to left ("forward") primer are underlined and **bold**. Due to the repetitive nature of sequences, several amplification products can be anticipated.

number: 452, 353, 299, 200, 146, and 47. PCR reactions were carried out with 500 ng DNA and regular Taq polymerase and involved 35×1 min cycles with temperatures of 94°C (denaturation), 61°C (annealing), and 72°C (extension).

Oxygen consumption measurements

VSMC were trypsinized, washed, and resuspended to a density of 4×10^6 cells/mL in PBS, pH 7.4. Immediately thereafter, VSMC were transferred to an air-tight chamber with continuous stirring and O_2 consumption was monitored using a computer-interfaced Clark electrode (Hansatech, Norfolk, UK) operating at 37°C, after previous calibration with sodium dithionite. Data were initially obtained over 3 min for each VSMC sample and compared with values obtained after subsequent incubation with oligomycin (20 μg/mL). The saturation oxygen concentration at this temperature was considered 210 μM (42), as informed by the manufacturer.

Assessment of ROS in VSMC

$O_2^{\cdot-}$ production was estimated using HPLC analysis of fluorescent dihydroethidium (DHE)-derived oxidation products, as described in detail previously (12). Briefly, VSMC were incubated with DHE (100 μM, 30 min, 37°C) in PBS/DTPA (diethylene triaminepentaacetic acid), 100 μM. After washing, cells were harvested in CH_3CN and dried. Pellets were resuspended in PBS for HPLC analysis, carried out using a C18 column with Photodyode Array Detector (Waters 2996, Milford, MA; for DHE) and fluorescence detectors.

Hydrogen peroxide production was assessed using an Amplex Red assay kit (Invitrogen). VSMC grown to $\sim2\times10^6$ cells in a 100 mm dish were incubated with 2 mL of HRP (10 U/mL) and Amplex Red reagent (250 μM) in PBS/EDTA 100 μM, pH 7.4, in the dark. Absorbance was analyzed serially in 200 μL aliquots of supernatant for up to 150 min, at 575 nm, using a Spectramax 340 spectrophotometer (Molecular Devices, Sunnyvale, CA).

NADPH oxidase activity

VSMC membrane homogenates were prepared as described previously (27), and protein concentration was assessed using the Bradford method. Cross-contamination between mitochondria and membrane fraction NADPH oxidase was ruled out on the basis of extensive validations performed previously in our and other laboratories (17, 27). Lucigenin chemiluminescence was performed in 20 μg membrane fraction protein aliquots as described in ref. 27, through incubation with lucigenin (5 μM) in PBS/EDTA and addition of NADPH (100 μM). Luminescence was monitored for 5 min using a Berthold 9505 luminometer at 37°C.

In addition, NADPH oxidase activity was also assessed by dihydroethidium fluorescence detected by HPLC, as described previously in detail (12). Briefly, VSMC membrane fractions (20 μg) were incubated with DHE (50 μM) in PBS/DTPA and NADPH (300 μM) (30 min, 37°C) and analyzed by HPLC under the same chromatographic conditions described above. Alternatively, experiments were performed using a microplate reader. Membrane fractions were incubated with DHE (10 μM) in PBS/DTPA in the presence of NADPH (50 μM) and DNA (1.25 μg/mL) for 30 min at 37°C, in the dark, and analyzed using microplate reader with rhodamine filter (excitation 490 nm, emission 590 nm).

Angiotensin II incubation protocol

VSMC were incubated with AngII at a final 100 nM concentration for 4 h, in the presence of 10% FBS. In EtBr-exposed VSMC, AngII incubation started after 20 h incubation and was maintained for an additional 4 h. All experiments were performed with simultaneous parallel runs for control and EtBr-exposed VSMC.

Nitrite and nitrate levels

Nitrite and nitrate levels were quantified in culture medium supernatants by chemiluminescence, using a Sievers NOA280 Analyzer (Boulder, CO), as described in ref. 29.

Superoxide dismutase activity

Total SOD activity was assessed in cell homogenates (10–15 μg protein) by inhibition of cytochrome-c reduction, as described in ref. 29.

Comet assay for nuclear DNA damage

VSMC ($\sim 8\times10^5$) were trypsinized, pelleted, and resuspended in 500 μL PBS. Cell suspension (20 μL) was added to 100 μL low-melting agarose at 37°C, and 90 μL were pipetted onto a slide precoated with 1% solution of normal melting point agarose. An additional agarose layer without cells was added after solidification of the first layer. After solidification, slides were placed in alkaline lysis solution in the dark at 4°C for 90 min, and later placed in fresh alkaline rinse solution for 20 min in a horizontal electrophoresis chamber. Subsequently, the slides were subjected to electrophoresis at 25 V/300 mA for 20 min. Following electrophoresis, slides were rinsed with neutralizing buffer 3X for 5 min, washed with 100% ethanol, stained with 50 μL ethidium bromide solution (20 μg/mL), and immediately examined on a blind fashion using an optical microscope Diaphot 300 (Nikon, Melville, NY) 510–560 nm/590 nm filter. A nuclear DNA damage score was calculated through observation of comet morphology (score 1–4) and cell number, as follows: [(comets class 1×0) + (comets class 2×1) + (comets class 3×2) + (comets class 4×3)].

MTT assays

MTT assays, usually used as a measurement of cell viability, reflect the activity of mitochondrial succinate dehydrogenase. VSMC (2×10^4 cells) were seeded and cultured for 24 h in a 96-well plate, followed by further incubation for 24 h in presence or absence of EtBr, while during the last 4 h MTT (3-(4,5-dimethylthiazol-2-yl)-2,5-diphenyltetrazolium bromide; 600 μM) was added. VSMC were then washed with PBS (pH 7.4), followed by DMSO, which solubilizes formazan crystals. Absorbance was measured at 570 nm.

Analysis of glutathione levels

Reduced glutathione (GSH) in total VSMC homogenates was analyzed by HPLC electrochemical detection (16) in a Waters system equipped with an electrochemical Model 247 (gold electrode) detector and 0.6 V applied potential. Chromatographic separation was carried out using X-Terra (4.5×250 mm; 5 μm particle size) column. The mobile phase (0.5 mL/min flow) was 100 mM KH_2PO_4 (pH 2.5), 200 mg/L sodium heptanosulfonate, 5 mg/L EDTA, and 1% methanol (vol/vol). GSH was identified and quantified by comparison with standard injections. Oxidized glutathione (GSSG) was calculated by subtraction of GSH levels from total glutathione, analyzed by enzymatic reduction to GSH with 0.6 U/mL glutathione reductase and 0.2 mg/mL NADPH for 30 min. The reaction was stopped by the addition of 10% TCA. After centrifugation at 11,000 g for 10 min at 4°C, the supernatants were injected into the HPLC system.

Real time PCR

Total RNA was purified from VSMC using a RNA spin isolation kit (GE Healthcare, Buckinghamshire, U.K.), according to the manufacturer's instructions. RNA from VSMC was reverse transcribed with Superscript II reverse transcriptase (Invitrogen). Message expression was quantified with the use of SYBR Green PCR Mix and the Rotorgene 6000 cycler (Corbett, Mortlake, New Australia) with Master Mix (Invitrogen) and specific rabbit Nox1 or Nox4 primers normalized to GADPH housekeeping. Primers were designed based on cloned sequences for rabbit Nox1 and Nox4, generously provided by Dr. Bernard Lassègue, from Emory University, Atlanta. Primer sequences were as follows:

forward Nox-1 (5′-GCTTCCGGATAAACTCCACA-3′); reverse Nox-1 (5′-CATCATGGGAAGGAAGGAGA-3′); forward Nox-4 (5′-TACTGGCCAGGTCTTGCTTT-3′); reverse Nox-4 (5′-CCACAGACTTGGCTTTGGAT-3′); forward GADPH (5′-TCACCATCTTCCAGGAGCGA-3′) and reverse GADPH (5′-CACAATGCCGAAGTGGTCGT-3′). The incubation conditions were: 95°C for 10 min, followed by 40 cycles of 15 s at 94°C, annealing for 15 s, at 60°C, and extension for 20 s at 72°C. Regular nonquantitative PCR in cells or arterial specimens was performed with the same parameters, except for a total of 35 cycles.

Vascular balloon injury

Vascular balloon injury was performed as described in detail previously (29) in the iliac artery of anesthesized normolipidemic rabbits, using a coronary-type angioplasty catheter inflated at 8 atmospheres, promoting profound arterial wall damage with rupture of internal elastic lamina. Arteries ($n = 4$) were analyzed 14 days after injury, with the contralateral uninjured iliac artery serving as control.

Western blot analysis

Proteins (30 μg) were separated in SDS-PAGE (12%) and fixed in nitrocellulose membrane. After blocking (nonfat milk

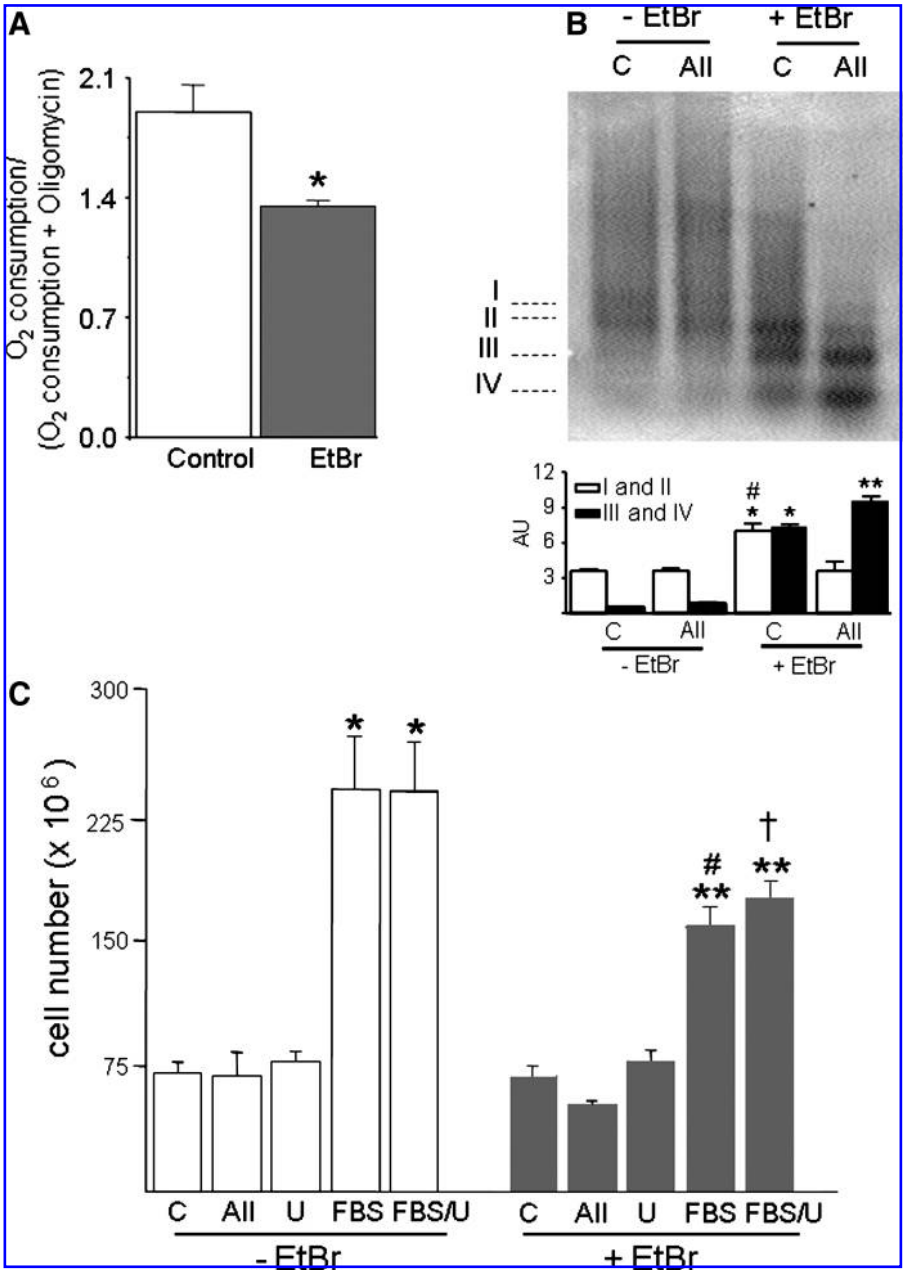

FIG. 2. Characterization of mitochondrial dysfunction induced by ethidium bromide (250 ng/mL for 24 h) in VSMC (pseudo-ρ° model). (**A**) Oxygen consumption measured with an oxygen electrode in whole trypsinized VSMC without and with EtBr. Data represent values obtained for each basal condition, normalized for oxygen consumption after inhibition with oligomycin 20 μg/mL, added subsequently in each sample ($n = 5$ experiments). (**B**) PCR amplification of D-loop second repetitive region with primers depicted in Fig. 1. Several unprecisely defined products are present in the absence of EtBr, whereas mtDNA damage after EtBr is evident by decrease of longer products and enhancement of smaller products defining individual bands. Representative of five independent experiments, which showed similar patterns. Densitometric analysis was performed at regions designated as I–IV. For simplification, the graph represents analysis of average values for I and II bands (*clear bars*) or III and IV bands (*dark bars*). (**C**) Quantitation of VSMC number after incubation for 72 h in F-12 media in presence or not of EtBr (250 ng/mL), containing different supplements or stimulus (C = F-12 without serum, AII = angiotensin II (100 nM/4 h), U = F-12 supplemented with uridine (50 μg/mL), and FBS = F-12 with 10% FBS). Values are mean ± SE ($n = 4$–6 experiments). *$p < 0.05$ *vs.* basal control (-EtBr); **$p < 0.05$ *vs.* EtBr control; $^{\#}p < 0.05$ *vs.* FBS (-EtBr), and †$p < 0.05$ *vs.* FBS/U (-EtBr).

5%, 2 h), membranes were incubated with anti-PDI or anti-KDEL primary antibody from Stressgen (AnnArbor, MI) and ABR (Dublin, OH), 1:1,000 or antibodies against phosphorylated or total p38MAPK (Cell Signaling, Danvers, MA), followed by HRP-conjugated secondary antibody (1:1,000, 1h). Immunoreactive bands were detected by chemiluminescence.

Statistical analysis

Values are expressed as mean ± standard error (SE). Statistical comparisons were performed with Student's *t*-test or one-way ANOVA followed by Student-Newman-Keuls multiple-range test, at a 0.05 significant level, using The Primer of Biostatistics, Stanton A. Glantz, version 3.01, McGraw-Hill, 1992.

Results

Characterization of mitochondrial dysfunction in pseudo-ρ^0 VSMC

Induction of mtDNA damage with the EtBr protocol described in Methods was associated with an average 29% decrease in oxygen consumption rate, confirming the expected minor compromise in mitochondrial energetic function (Fig. 2A).

Assessment of mtDNA damage through PCR amplification of second repetitive sequence region of D-loop (see Methods) showed (Fig. 2B) in control VSMC an expected smear composed of multiple unprecisely defined bands indicative of amplification of several products in the expected region between 200 and 460 kb. Such a pattern was not visibly altered

after AngII in control VSMC. In VSMC incubated with EtBr for 24 h, there was less amplification of the larger products and predominant amplification of smaller products ~140–200 bp, which formed more defined bands. Interestingly, this pattern was consistently and uniformly enhanced after incubation with AngII ($n = 5$, Fig. 2B). These results confirm the occurrence of mtDNA damage induced by EtBr and its likely increase by AngII under this condition.

Cell number did not change after 24 h EtBr incubation, with no apparent morphological changes in EtBr-exposed VSMC. In addition, the pseudo-ρ^0 VSMC were viable, as documented by Trypan Blue exclusion (not shown). MTT reduction assays showed average decrease of $14 \pm 6\%$ ($n = 5$, $p < 0.05$), which (given the absence of cell death) is further indicative of mitochondrial dysfunction at the level of succinate dehydrogenase activity. To further examine physiological consequences of EtBr incubation for a more prolonged period (72 h), we performed cell number quantitation assays (Fig. 2C). AngII incubation in this protocol did not lead to cell number change. In the presence of 10% FBS, there was an expected increase in cell number, whereas EtBr-exposed cells showed 28% decrease in cell population after 72 h (Fig. 2C), with no evidence either of cell death or expression of a senescence marker such as p21 (not shown).

Together, these results indicate that our protocol of EtBr incubation induced mild mitochondrial dysfunction, which did not compromise cell viability. Growth limitation was detectable only after an EtBr exposure time beyond that in which we performed the NADPH oxidase assays described in subsequent experiments.

Baseline ROS generation in pseudo-ρ^0 VSMC

Accumulation of mtDNA mutations leading to respiratory chain dysfunction are well known to promote ROS generation (54). We thus assessed ROS production after EtBr incubation. As expected from the mild nature of induced dysfunction discussed above, assessment of ROS production by HPLC analysis of DHE-derived products yielded no changes in 2-hydroxyethidium adduct (indicative of superoxide) and minor nonsignificant increase in ethidium adduct (indirectly reflecting hydrogen peroxide and other oxidants) (12) (Fig. 3A). Assessment of basal hydrogen peroxide steady-state generation by Amplex Red® assay showed a small (average 16%) significant increase after EtBr exposure (Fig. 3B). We cannot exclude that the observed moderate increase in Nox4 levels (see below) may have contributed to this hydrogen peroxide production, considering that this isoform generates predominantly hydrogen peroxide (26). Thus, our protocol of EtBr exposure did not lead to massive changes in VSMC ROS production which might induce unrealistic alterations in secondary targets.

To assess whether the EtBr concentration used in our study promoted significant disruption of nuclear DNA, we performed comet assays. Results (Fig. 3C) showed a concentration-dependent increase in the score of comet formation. However, at the concentration used in our study (250 ng/mL), only minor nonsignificant changes were seen and in no instance we detected comets beyond class 1-2.

To document possible physiological effects of mtDNA damage in our model, we assessed phosphorylation of p38 MAPK after EtBr exposure. Figure 3D shows increase in p38 MAPK phosphorylation after EtBr and its decrease by concomitant 24 h incubation with PEG-SOD + PEG-catalase (20 and 150 U/mL, respectively).

VSMC redox status, SOD activity, and nitrogen oxide levels

In order to further characterize possible factors that could affect secondary targets such as NADPH oxidase in our pseudo-ρ^0 VSMC, we performed measurements of cell redox status and other variables. Our results show that EtBr exposure did not induce detectable changes in GSH/GSSG ratio (Fig. 4A), total SOD activity (Fig. 4B), and levels of nitrogen oxides. Also, AngII induced no change in SOD activity and nitrogen oxide levels (Fig. 4C and D).

Effects of mild mitochondrial dysfunction on NADPH oxidase activity after AngII

To investigate possible upstream effects of mitochondria on NADPH oxidase, we first measured NADPH oxidase activity in VSMC membrane fraction using distinct techniques. In control VSMC, incubation with Ang II (100 n*M*, 4 h) induced the expected increase in NADPH oxidase activity, assessed both by lucigenin chemiluminescence (Fig. 5A) or HPLC analysis of fluorescent DHE-derived products (Fig. 5B). Importantly, in VSMC exposed to EtBr for 24 h, the NADPH oxidase response to AngII was completely abrogated, as assessed by either method, while there was also a baseline decrease in 2-EOH product (Fig. 5B). Analogous results were observed after 72 h of EtBr incubation (Fig. 5C). Figure 5D summarizes percent changes in NADPH oxidase activity with AngII. Interestingly, the increased baseline phosphorylation of p38MAPK after EtBr incubation was decreased by AngII (Fig. 3D).

Because it is difficult to fully exclude that EtBr promoted damage in nuclear DNA, which might have influenced our results, we also performed NADPH oxidase activity assays (using an HPLC/DHE technique) in membranes from VSMC that were incubated with the specific complex III inhibitor antimycin A (100 n*M*) for 24 h. This concentration was selected to promote an average 21% decrease in oxygen consumption, thus matching the changes induced by EtBr. Such antimycin A incubation also promoted a nearly identical pattern of decreased oxidase activation due to AngII (Fig. 5E).

Expression of Nox isoform mRNA after mitochondrial dysfunction

Regular nonquantitative PCR (Fig. 6A) showed that after EtBr there was a decrease in Nox1 expression and appearance of a clear band for an amplified Nox4 product. This suggested that loss in AngII responsiveness after mitochondrial dysfunction could be at least in part due to changes in expression of Nox isoforms, since in VSMC Nox1 is well known to be induced, while Nox4 is unchanged or inhibited by AngII (9, 26). We therefore performed further experiments with real-time quantitative PCR (Figs. 6B and C). In VSMC not exposed to EtBr, we observed significant 2.3-fold increase in Nox1 mRNA expression, while Nox4 mRNA was unchanged or decreased after AngII. After EtBr incubation for 24 h, there was a significant baseline 1.6-fold increase in Nox4 mRNA

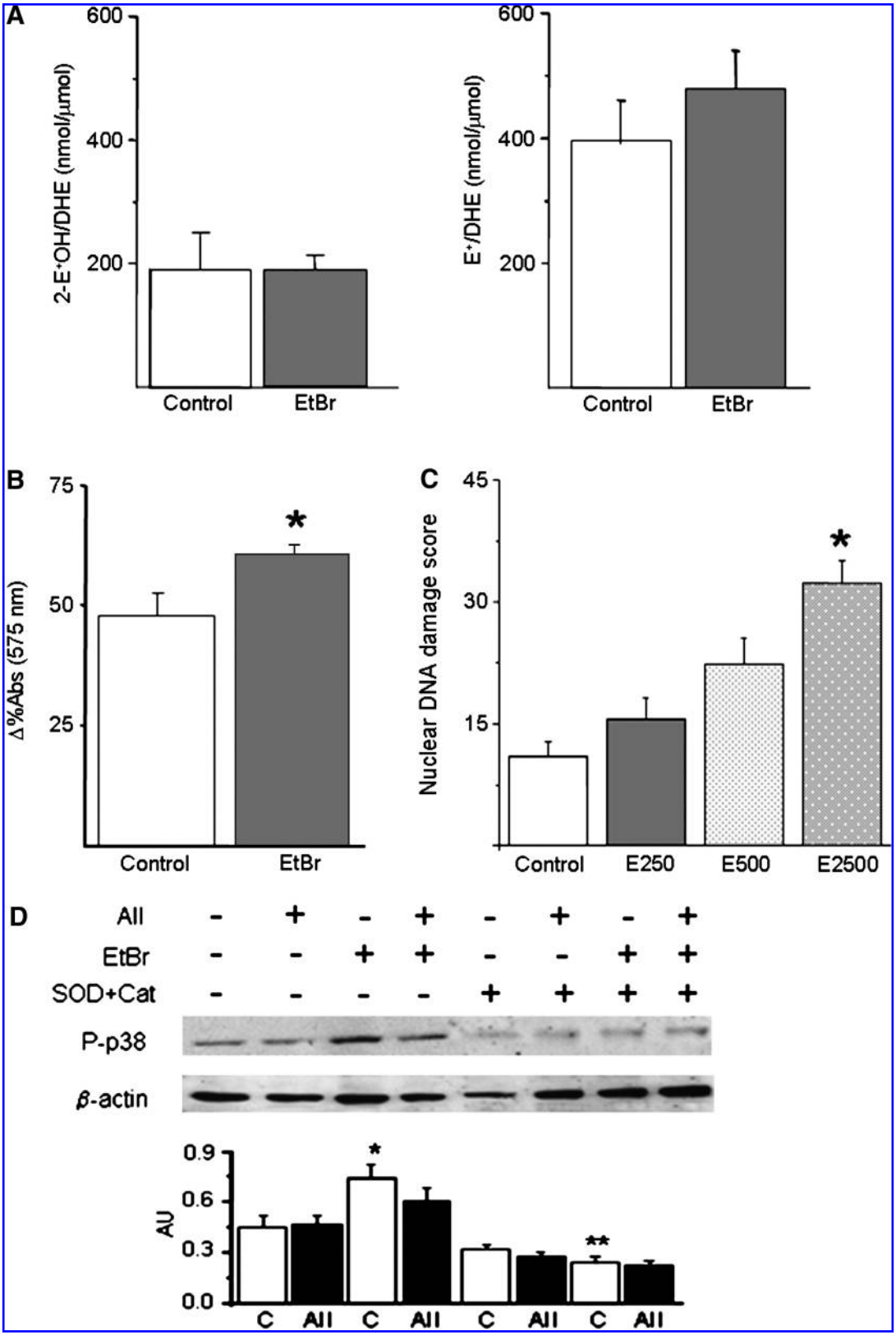

FIG. 3. Characteristics of pseudo-ρ° VSMC. In (**A**) and (**B**): Analysis of ROS production in control and pseudo-ρ° VSMC. (**A**) HPLC analysis of dihydroethidium oxidation products 2-hydroxyethidum (=2-E^+OH, *left graph*) and ethidium (=E^+, *right graph*). (**B**) Hydrogen peroxide production detected by Amplex Red® in control and pseudo-ρ° VSMC. (**C**) Comet assay for investigation of nuclear DNA damage in control VSMC and in VSMC incubated with EtBr for 24 h in concentrations ranging from 250 to 2500 ng/mL. Results from three independent experiments are expressed as a score calculated from number of cells *vs.* severity of comet formation (see Methods section) and analyzed by ANOVA with SNK multiple-range test. (**D**) Western blot analysis and densitometric analysis depicting phosphorylation of p38MAPK and effects of ethidium bromide (24 h) incubation in presence or absence of PEG-SOD (20 U/mL) + PEG-catalase (150 U/mL).Values are mean ± SE ($n = 3$ independent experiments). *$p < 0.05$ *vs.* control.

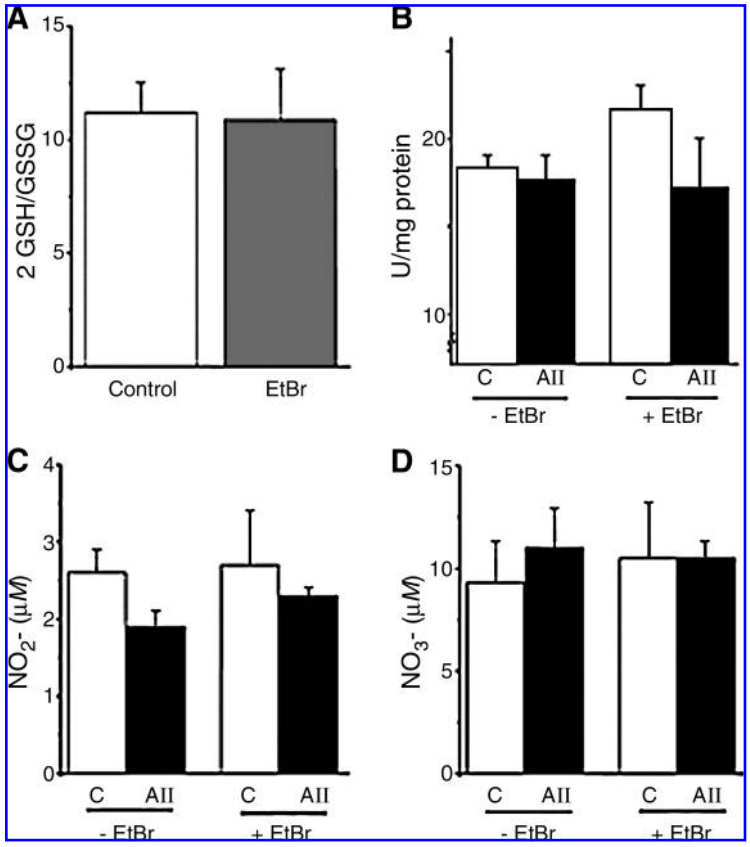

FIG. 4. Cellular redox status in VSMC with mitochondrial dysfunction. (**A**) Analysis of intracellular GSH/GSSG ratio in homogenates of control and pseudo-ρ° VSMC, by HPLC and electrochemical detection. (**B**) SOD activity in VSMC and pseudo-ρ° VSMC homogenates, assessed through inhibition of cytochrome-c reduction ($\varepsilon_{550nm} = 2.1 \times 10^4 M^{-1}\ s^{-1}$). (**C**) and (**D**) depict analysis of nitrite and nitrate levels, respectively, in culture media of VSMC and pseudo-ρ° VSMC by chemiluminescence. Values are mean ± SE ($n = 3$–6 experiments). AU, arbitrary units.

and a nonsignificant increase in Nox1 mRNA. Moreover, after AngII, Nox1 mRNA showed negligible further increase, while Nox4 mRNA showed minor decrease. In a similar fashion, incubation of VSMC with antimycin A for 24 h promoted no significant change in baseline Nox1 mRNA expression (Fig. 5D), *versus* a 1.8-fold increase in Nox4 mRNA (Fig. 5E).

Changes in endoplasmic reticulum stress markers and protein disulfide isomerase (PDI) expression and migration pattern

To assess whether increased Nox4 expression was due to endoplasmic reticulum stress, a condition described to induce Nox4 in VSMC (40), we assessed endoplasmic reticulum stress markers after EtBr incubation. Mitochondrial dysfunction induced variable and small changes in expression of chaperone markers (Fig. 7A), clearly distinct than the marked increases obtained with the classical endoplasmic reticulum stressor tunicamycin (not shown). PDI was recently described by our laboratory to act as a regulatory protein associated with NADPH oxidase (18). PDI is sensitive to stress conditions such as hypoxia (45). We therefore assessed PDI expression after mitochondrial dysfunction. As shown in Fig. 7B, there was increase in total PDI expression and, in addition, an inversion in the pattern of PDI migration to membrane. As we showed before (18), PDI migrates to membrane during AngII exposure. After EtBr incubation, PDI showed important baseline migration to membrane fraction and a decrease with AngII. In addition, a second band was evident for PDI after EtBr, the origin of which is unclear at present.

Evidence for mtDNA damage during vascular repair after injury

To gather evidence of mtDNA injury in a context involving VSMC pathophysiology, we assessed (by RT-PCR) transcripts for NADH dehydrogenase 1 (NADH1) or cytochrome-c oxidase 2 (COX2) from rabbit iliac arteries submitted to overdistention balloon injury 14 days before or from contralateral uninjured arteries (control). Our results show a failure of amplification of NADH1, but not COX2 transcripts, in injured but not control arteries. This indicates a selective, rather than widespread, pattern of mtDNA damage. Interestingly, failure of NADH1 amplification was also seen in HEK293 cells incubated with EtBr (see description in Methods).

Discussion

A major finding of our study was that mild mitochondrial dysfunction induced by forced mtDNA mutations totally abrogated membrane NADPH oxidase activation due to AngII. Such effect was due at least in part to associated changes in the expression of AngII-responsive Nox(es), with decrease in Nox1 and increased baseline expression of AngII-insensitive Nox4. Such evidence that integrity of mitochondrial function is required for efficient AngII-mediated activation of NADPH oxidase has pathophysiological implications for understanding regulation and compartmentation of enzymatic ROS sources during redox cell signaling.

A basic question regarding the proposed cross-talk between mitochondria and NADPH oxidase is the specificity of pathway(s) connecting both ROS-generating systems. In this

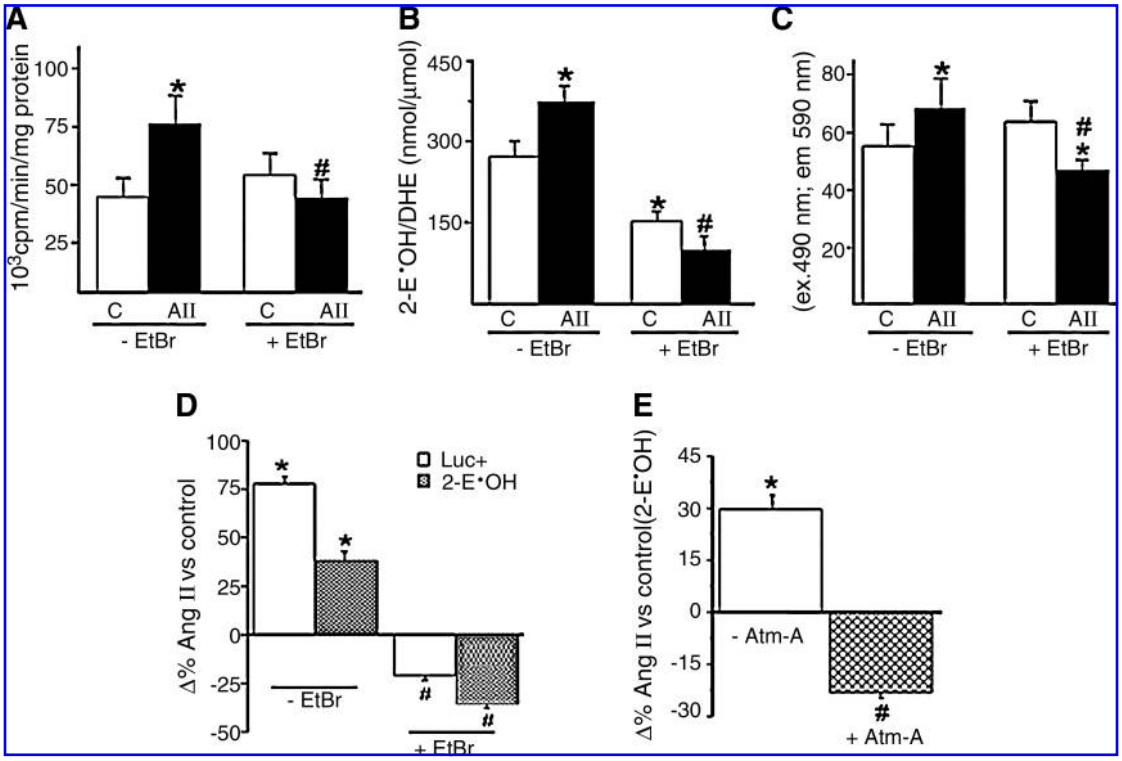

FIG. 5. NADPH oxidase activity assays in membrane fraction of control and pseudo-ρ° VSMC, in baseline control condition (C) and after incubation with AngII (AII, 100 n*M*/4 h). (**A**) Measurement by lucigenin chemiluminescence. Membrane fractions (20 μg protein) were added to 1 mL of PBS at 37°C, followed by lucigenin (final concentration 5 μM) and NADPH (100 μM); luminescence was recorded for 5 min. (**B**) Measurement by HPLC analysis of DHE oxidation products. Membrane fractions (20 μg) were incubated with DHE (50 μM) in PBS/DTPA in the presence of NADPH (300 μM) for 30 min at 37°C, and analyzed by HPLC. Graph shows quantification of 2-E^+OH formed/DHE consumed (see ref. 12). (**C**) Similar to (**B**), after 72 h of prior EtBr incubation. Here, DHE product (mainly 2-E^+OH, see Ref. 12) was quantified in microplate reader under rhodamine filter (excitation 490 nm, emission 590 nm). (**D**) Summary of percent changes in NADPH oxidase activity with AngII in absence or presence of prior EtBr incubation. (**E**) Summary of percent changes in membrane fraction NADPH oxidase activity with AngII in the absence or presence of antimycin A (Atm-A, 100 n*M*, 24 h incubation). Values are mean ± SE ($n = 3$–4 independent experiments). *$p < 0.05$ *vs.* C–EtBr or C–Atm-A, #$p < 0.05$ *vs.* AII-EtBr or AII–Atm-A).

context, our model provided a relatively clean tool to unravel an upstream effect of mitochondria on NADPH oxidase. The transient character and low degree of exposure to ethidium bromide or antimycin A in our cells minimized chances of secondary effects of long-term mitochondrial dysfunction, such as apoptosis, cell senescence, and nonspecific responses to stress or to extreme metabolic changes. Thus, our data are consistent with the possibility of direct signaling pathway(s) for a cross-talk between NADPH oxidase and mitochondria. Still, at least a few such pathways affecting NADPH oxidase may merge with physiological programs such as differentiation, metabolic adaptations, and hypoxic signaling, as detailed in the discussion below, in the context of signaling response(s) to minor cell stress, which is intrinsic to even low-degree mitochondrial dysfunction (38, 54). While such signaling routes are likely to display physiological and pathophysiological significance, a more complete assessment of their structure and specificity requires further study.

Our EtBr model, while being essentially artificial, clearly reproduces a general form of mild mitochondrial dysfunction, as indeed further evidenced by its similarities with antimycin A exposure. Such mitochondrial dysfunction has been documented in a host of pathophysiological situations, which almost invariably also depict activation of NADPH oxidases (8, 20, 24, 26, 33). On the other hand, our model has some indirect bearings in several pathophysiological situations in which mtDNA mutations have been demonstrated, including aging (54), atherosclerosis (3), and diabetes (54). Interestingly, we were able to document evidence for mtDNA damage during vascular repair after injury (Fig. 7C). Considering the multiple copies of mtDNA per cell and that function appears to be importantly compromised only after 90% of mtDNA is mutated in each cell (22, 23), there is an ongoing debate as to whether mtDNA mutations in such diseases can indeed account for further cell damage or are just a consequence of increased ROS levels (55). In this regard, it is important to consider that mitochondrial superoxide production (53), mitochondrial dysfunction (38), aging (2), and possibly also mtDNA mutations (54) are all highly stochastic events, which may thus produce a nonuniform cell-specific pattern of damage within a given cell population. Such considerations indicate that extrapolation of this model to represent diseases in which mtDNA mutations are known to occur may be oversimplistic.

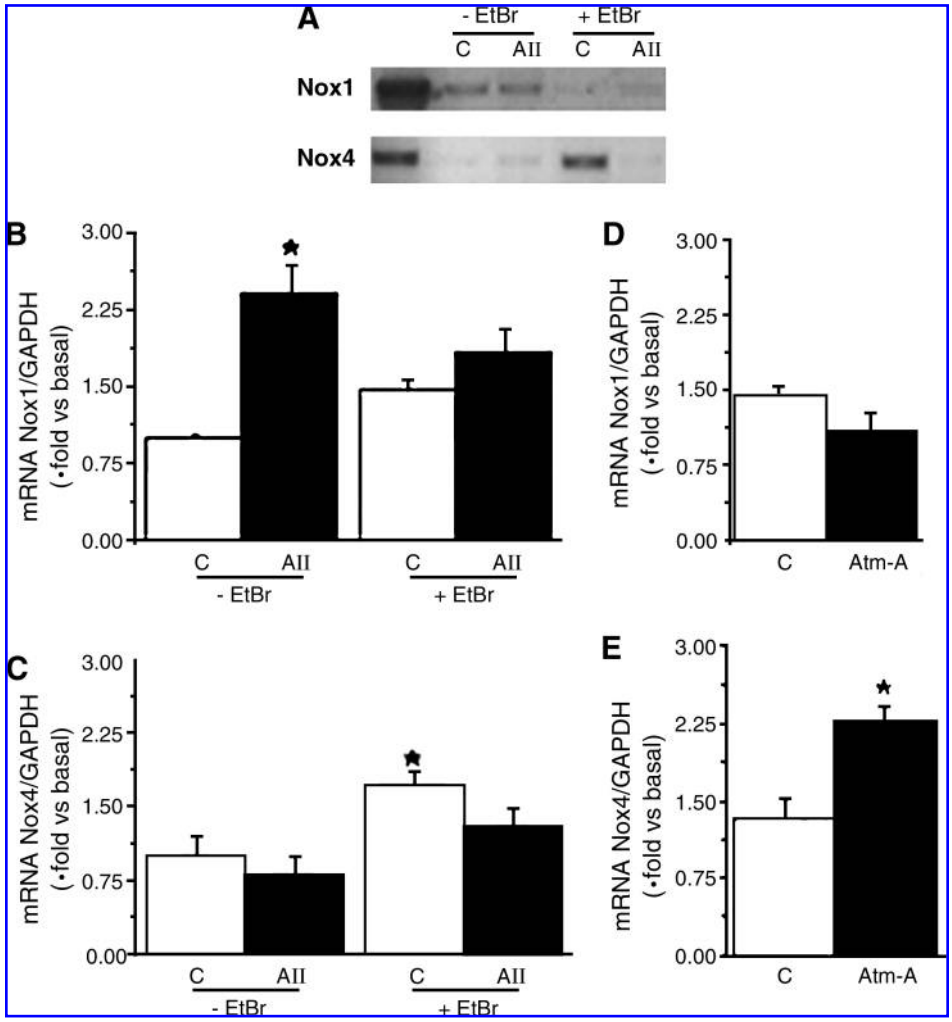

FIG. 6. Assessment of mRNA for NADPH oxidase isoforms by PCR. (**A**) Regular nonquantitative RT-PCR for amplification of Nox1 and Nox4 mRNA. *Left lanes* are standards obtained from plasmid amplification. (**B**) and (**C**) Real-time quantitative RT-PCR for Nox1 and Nox4 mRNA amplification in VSMC in control condition or after exposure to EtBr for 24 h, in response to AngII incubation. (**D**) and (**E**) Real-time quantitative RT-PCR for Nox1 and Nox4 mRNA amplification in VSMC in control condition or after exposure to Antimycin A (100 n*M* for 24 h). Data were normalized for housekeeping GAPDH mRNA. Values are mean ± SE ($n = 3$ experiments). *$p < 0.05$ *vs.* basal control.

Since Nox1 is the major AngII-responsive Nox in VSMC (9, 26), including the rabbit cells used in our study (18), the observed failure to upregulate Nox1 after mitochondrial dysfunction likely dominated the loss of AngII-mediated increase in NADPH oxidase activity. Furthermore, mitochondrial-dependent pathways promoted clear increase in Nox4 mRNA expression. The later result adds novel information on Nox4 regulatory mechanisms, which have proven difficult to contextualize (24), suggesting that this isoform can be induced even by relatively minor stresses, in line with its postulated role of stress-inducible Nox (24). Whether Nox4 mRNA expression occurs through pathways in common with those mediating cell differentiation or adaptation to hypoxia—conditions known to involve both mitochondria and Nox4 (39)—deserves further investigation. On the other hand, markers of endoplasmic reticulum stress, known to trigger Nox4 (40), were unaltered in our model. Knowledge of Nox protein levels after mitochondrial dysfunction, although important, is hampered by difficulties regarding antibody specificity. Although our work showed that decreased response to AngII is concomitant to increased Nox4 mRNA, AngII may trigger Nox4 in cell types such as mesangial cells (24) and even VSMC after serum starvation at higher AngII concentrations (unpublished observations from our laboratory). Therefore, although the interaction between mitochondria and NADPH oxidase may hold true for many different cells, its consequences regarding redox signaling may depend on specific conditions and cell type. In addition, our ongoing investigations showed that increases in NADPH oxidase activity promoted by the endoplasmic reticulum stressor tunicamycin are also abrogated by induced mtDNA mutations (unpublished data), suggesting that the cross-talk proposed in our study is a more general phenomenon, independent of signaling events specific only to AngII pathways.

Mechanisms whereby mitochondria communicate with NADPH oxidase can reflect distinct, possibly inter-related aspects of mitochondrial function, including ROS production, energy metabolism, and calcium homeostasis. It is well known that exogenous ROS can induce expression and activity of Nox(es), particularly Nox4 in our VSMC (31, 32, 34). However, incubation of VSMC with catalase (100 units/mL, starting 12 h before EtBr) did not prevent the observed changes in Nox isoform mRNA (data not shown), indicating that cytoplasmic ROS increase may not be sufficiently intense or sustained to affect Nox. It cannot be excluded, however, that ROS in specific compartments (including mitochondria) or other reactive species might have contributed to the observed Nox changes. Second, metabolic changes induced by dysfunctional mitochondria could potentially be involved in NADPH oxidase modulation. The observed redox-dependent

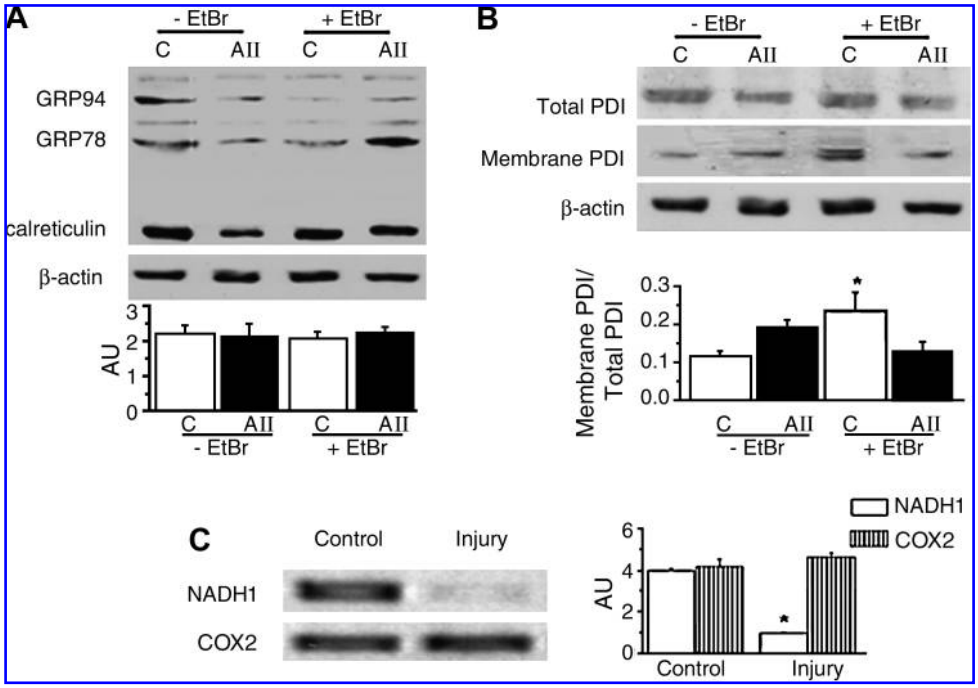

FIG. 7. Expression of endoplasmic reticulum stress markers and PDI in VSMC under control conditions and after incubation with EtBr for 24 h. (**A**) Western blot analysis and densitometry depicting expression of chaperones GRP78, GRP 94, or calreticulin, analyzed with anti-KDEL antibody, in control VSMC and after incubation with EtBr for 24 h, in response to AngII (AII). (**B**) Western blot analysis and densitometry depicting PDI expression in total homogenates or membrane fraction at baseline and after incubations with EtBr for 24 h, in response to AngII. Densitometry expresses ratio between membrane fraction/total PDI. (**A**) and (**B**) represent data from 3 to 5 independent experiments each. (**C**) RT-PCR amplification of transcripts of mtDNA obtained from RNA extracted and reverse-transcribed from rabbit iliac arteries submitted to overdistention balloon injury 14 days before or from contralateral uninjured arteries (control). Primer sequences were similar to those depicted in Fig. 1A for NADH dehydrogenase 1 (NADH1) or cytochrome-c oxidase 2 (COX2). *Left panel* depicts representative example, while the *right graph* is a summary analysis of 4 independent experiments. $^*p < 0.05$ *vs*. control; mean ± SE.

phosphorylation of p38MAPK indicates not only a documented physiological consequence of mtDNA damage, but also a potential pathway mediating metabolic changes typically associated with nutrient deprivation (21). Also, the metabolic kinase 5′AMP-activated protein kinase (AMPK), known to be activated by mitochondrial-derived oxidants (60), reportedly suppress NADPH oxidase activation in endothelial cells (60) and inhibits AngII-mediated VSMC proliferation (36). Together, these data suggest a possible role for metabolism alterations in the cross-talk between mitochondria and NADPH oxidase. Finally, disturbed calcium homeostasis could potentially underlie activation of Nox(es), while amplifying mitochondrial ROS generation (49). Another condition potentially involved in our model is the recently described stress response due to mitochondria-specific protein misfolding (56). This signaling cascade leads to increased mitochondrial chaperone expression, which is dependent on proapoptotic transcription factors (56). In addition to mitochondrial pathways, cross-talk with Nox(es) can also be mediated by some kinases and phosphatases that are upstream of growth factor-mediated Nox activation (26) and could potentially sense mitochondrial dysfunction. Indeed, transactivation of growth factor receptors, known to be involved in Nox signaling (9, 26), is also influenced by mitochondrial function (7, 28). Furthermore, changes in NADPH oxidase after mitochondrial dysfunction were associated with increased expression and an inverted pattern of migration of PDI to membrane fraction. PDI, known to be involved in intracellular protein traffic (47), associates with NADPH oxidase and regulates its function, while migrating to membrane fraction during oxidase activation (18). Given that traffic to membranes is essential for oxidase activation (48), these results raise the hypothesis of PDI involvement in mitochondrial cross-talk with NADPH oxidase, although pathways underlying PDI interaction with NADPH oxidase remain under investigation. Finally, although we focused on functional aspects of the cross-talk between mitochondria and Nox(es), the possibility of a physical cross-talk cannot be ruled out, considering a previous report in tumor cells showing Nox1 localization at mitochondrial surface (10). In our VSMC, such evidence was not sufficiently clear, although we did see some degree of co-localization between Nox4 and mitochondria at the perinuclear region (unpublished results). However, given the low specificity of available antibodies against Nox(es), these results are not undisputed.

Previous reports indicated that interactions between mitochondria and NADPH oxidase can occur in both directions (10, 11). Our work thus reinforces such results and points to novel aspects of an upstream effect of mitochondria on NADPH oxidase. Altogether, it is likely that such interaction significantly affects redox-dependent cell signaling and may thus play a role in the pathogenesis of aging, as well as several diseases involving both mitochondrial dysfunction and NADPH oxidase, including atherosclerosis (3). In this context, the finding of mtDNA damage during vascular repair (Fig. 7C) is interesting, given the increased ROS production and expression of Nox1 and Nox4 previously documented in this model (30, 43). Of note, increased expression and activity of mitochondrial transcription factor (mtTFA) was shown to support neointima formation (52). In a lower scale, cross-talk between mitochondria and Nox(es) could mediate signaling associated with oxygen sensing, biomechanical

transduction, or cell differentiation. Indeed, both NADPH oxidases and mitochondria have been reportedly involved in all such conditions (26). An interesting observation was the consistently observed increase in mtDNA damage indicators when AngII was administered to cells with already dysfunctional mitochondria, but not to normal cells. We speculate that mitochondrial dysfunction might act as a switch from physiological to pathological AngII effects, a proposal in line with a prior report of AngII-induced mitochondrial ROS and dysfunction in endothelial cells (11).

In conclusion, our observations point out that events leading to mitochondrial dysfunction have significant upstream impact into NADPH oxidase activity and isoform expression. Such a novel aspect of this cross-talk may have significant implication for understanding disease mechanisms and for designing rational therapeutic interventions aimed at restoring redox homeostasis.

Acknowledgments

We are indebted to: Bernard Lassègue, from Emory University, Atlanta, Georgia, for providing rabbit sequences of Nox1 and Nox4 and for helping to establish real-time PCR; Roger Chammas, from U. São Paulo, for help with D-loop experiments; Judith Haendeler, from U. of Duesseldorf, for essential advice on the model; Ana Lucia Garippo, for assistance in some experiments; Thais Rodrigues Barbosa, for help with vascular injury experiments; Camille Caldeira and Erich Tahara, from Chemistry Inst., U. São Paulo, for assistance in experiments with mitochondrial oxygen consumption.

The research was supported by: Fundação de Amparo à Pesquisa do Estado de São Paulo, Conselho Nacional de Desenvolvimento Científico e Tecnológico (*Redoxoma* Millenium Institute), Financiadora de Estudos e Projetos.

Abbreviations

AMPK, 5′AMP-activated protein kinase; AngII, angiotensin II; Atm-A, antimycin A; COX2, cytochrome-c oxidase 2; DHE, dihydroethidium; D-Loop, displacement loop; DTPA, diethylene triaminepentaacetic acid; EDTA, ethylene diamine tetracetic acid; 2-EOH, 2-hydroxyethidium; EtBr, ethidium bromide; FBS, fetal bovine serum; GRP, glucose regulated proteins; GSH, reduced glutathione; GSSG, oxidized glutathione; HEK293, human embryonic kidney 293 cells; HPLC, high performance liquid chromatography; mtDNA, mitochondrial DNA; MTT, (3-(4,5-dimethylthiazol-2-yl)-2,5-diphenyltetrazolium bromide; NADH1, NADH dehydrogenase 1; Nox, nonphagocytic oxidase; PDI, protein disulfide isomerase; ROS, reactive oxygen species; SOD, superoxide dismutase; TCA, trichloroacetic acid; Tun, tunicamycin, VSMC, vascular smooth muscle cell.

Disclosure Statement

No competing financial interests exist.

References

1. Armand R, Channon JY, Kintner J, White KA, Miselis KA, Perez RP, and Lewis LD. The effects of ethidium bromide induced loss of mitochondrial DNA on mitochondrial phenotype and ultrastructure in a human leukemia T-cell line (MOLT-4 cells). *Toxicol Appl Pharmacol* 196: 68–79, 2004.
2. Bahar R, Hartmann CH, Rodriguez KA, Denny AD, Busuttil RA, Dollé ME, Calder RB, Chisholm GB, Pollock BH, Klein CA, and Vijg J. Increased cell-to-cell variation in gene expression in ageing mouse heart. *Nature* 441: 1011–1014, 2006.
3. Ballinger SW, Patterson C, Knight–Lozano CA, Burow DL, Conklin CA, Hu Z, Reuf J, Horaist C, Lebovitz R, Hunter GC, McIntyre K, and Runge MS. Mitochondrial integrity and function in atherogenesis. *Circulation* 106: 544–549, 2002.
4. Barthelemy C, De Baulny HO, and Lombes A. D-loop mutations in mitochondrial DNA: Link with mitochondrial DNA depletion? *Hum Genet* 110: 479–487, 2002.
5. Buonassissi V and Venter JC. Hormone and neurotransmitter receptors in an established vascular endothelial cell line. *Proc Natl Acad Sci USA* 73: 1612–1616, 1976.
6. Chandel NS and Schumacker PT. Cells depleted of mitochondrial DNA (rho0) yield insight into physiological mechanisms. *FEBS Lett* 454:173–176. Review. 1999
7. Chen K, Thomas SR, Albano A, Murphy MP, and Keaney JF. Mitochondrial function is required for hydrogen peroxide-induced growth factor receptor transactivation and downstream signaling. *J Biol Chem* 279: 35079–35086, 2004.
8. Chomyn A and Attardi G. MtDNA mutations in aging and apoptosis. *Biochem Biophys Res Commun* 304: 519–529, 2003.
9. Clempus RE and Griendling KK. Reactive oxygen species signaling in vascular smooth muscle cells. *Cardiovasc Res* 71: 216–225, 2006.
10. Desouki MM, Kulawiec M, Bansal S, Das GM, and Singh KK. Cross talk between mitochondria and superoxide generating NADPH oxidase in breast and ovarian tumors. *Cancer Biol Ther* 4: 1367–1373, 2005.
11. Doughan AK, Harrison DG, and Dikalov SI. Molecular mechanisms of angiotensin II mediated mitochondrial dysfunction. Linking mitochondrial oxidative damage and vascular endothelial dysfunction. *Circ Res* 102: 488–496, 2008.
12. Fernandes DC, Wosniak J Jr, Betoline M, Liberman M, Laurindo FR, and Santos CXC. Analysis of DHE-derived oxidation products by HPLC in the assessment of superoxide production and NADPH oxidase activity in vascular systems. *Am J Physiol Cell Physiol* 292: C413–C422, 2007.
13. Fish J, Raule N, and Attardi G. Discovery of a major D-loop replication origin reveals two modes of human mtDNA synthesis. *Science* 306: 2098–2101, 2004.
14. Guarente L. Mitochondria—a nexus for aging, calorie restriction, and sirtuins? *Cell* 132: 171–176, 2008.
15. Hansen JM, Go YM, and Jones DP. Nuclear and mitochondrial compartmentation of oxidative stress and redox signaling. *Annu Rev Pharmacol Toxicol* 46: 215–234, 2006.
16. Hiraku Y, Murata M, and Kawanishi S. Determination of intracellular glutathione and thiols by high performance liquid chromatography with a gold electrode at the femtomole level: comparison with a spectroscopic assay. *Biochim Biophys Acta* 1570: 47–52, 2002.
17. Janiszewski M, Souza HP, Liu X, Pedro MA, Zweier JL, and Laurindo FR. Overestimation of NADH-driven vascular oxidase activity due to lucigenin artifacts. *Free Radic Biol Med* 32: 446–453, 2002.
18. Janiszewski M, Lopes LR, Carmo AO, Pedro MA, Brandes RP, Santos CX, and Laurindo FR. Regulation of NAD(P)H oxidase by associated protein disulfide isomerase in vascular smooth muscle cells. *J Biol Chem* 280: 40813–40819, 2005.
19. Kasamatsu H, Robberson DL, and Vinograd J. A novel closed-circular mitochondrial DNA with properties of a replicating intermediate. *Proc Nat Acad Sci USA* 68: 2252–2257, 1971.

20. Kim JA, Wei Y, and Sowers JR. Role of mitochondrial dysfunction in insulin resistance. *Circ Res* 102: 401–414, 2008.
21. Kim JS, Saengsirisuwan V, Sloniger JA, Teachey MK, and Henriksen EJ. Oxidant stress and skeletal muscle glucose transport: Roles of insulin signaling and p38 MAPK. *Free Radic Biol Med* 41: 818–824, 2006.
22. King M and Attardi G. Human cells lacking mtDNA: Repopulation with exogenous mitochondria by complementation. *Science* 246: 500–503, 1989.
23. King MP and Attardi G. Isolation of human cell lines lacking mitochondrial DNA. *Methods Enzymol* 264: 304–313, 1996.
24. Krause KH Aging: A revisited theory based on free radicals generated by NOX family NADPH oxidases. *Exp Gerontol* 42: 256–262, 2007.
25. Lalucque H and Silar P. NADPH oxidase: An enzyme for multicellularity? *Trends Microbiol* 11: 9–12, 2003.
26. Lassègue B and Clempus RE. Vascular NAD(P)H oxidases: Specific features, expression, and regulation. *Am J Physiol Regul Integr Comp Physiol* 285: R277–R297, 2003.
27. Laurindo FR, Souza HP, Pedro M de A, and Janiszewski M. Redox aspects of vascular response to injury. *Methods Enzymol* 352: 432–454, 2002.
28. Lee SB, Bae IH, Bae YS, and Um HD. Link between mitochondria and NADPH oxidase 1 isozyme for the sustained production of reactive oxygen species and cell death. *J Biol Chem* 281: 36228–36235, 2006.
29. Leite PF, Danilovic A, Moriel P, Dantas K, Marklund S, Dantas AP, and Laurindo FR. Sustained decrease in superoxide dismutase activity underlies constrictive remodeling after balloon injury in rabbits. *Arterioscler Thromb Vasc Biol* 23: 2197–2202, 2003.
30. Leite PF, Liberman M, Sandoli de Brito F, and Laurindo FR. Redox processes underlying the vascular repair reaction. *World J Surg* 28: 331–336, 2004.
31. Li WG, Miller FJ Jr, Zhang HJ, Spitz DR, Oberley LW, and Weintraub NL. Enhanced H2O2-induced O2- production by a non-phagocytic NAD(P)H oxidase causes oxidant injury. *J Biol Chem* 276: 29251–29256, 2001.
32. Liberman M, Bassi E, Martinatti MK, Lario FC, Wosniak Jr J, Pomerantzeff PM, and Laurindo FR. Oxidant generation predominates around calcifying foci and enhances progression of aortic valve calcification. *Arterioscler Thromb Vasc Biol* 28: 463–470, 2007.
33. Madamanchi NR and Runge MS. Mitochondrial dysfunction in atherosclerosis. *Circ Res* 100: 460–473, 2007.
34. Martyn KD, Frederick LM, Von Loehneysen K, Dinauer MC, and Knaus UG. Functional analysis of Nox4 reveals unique characteristics compared to other NADPH oxidases. *Cell Signal* 18: 69–82, 2006.
35. Miller FJ Jr, Filali M, Huss GJ, Stanic B, Chamseddine A, Barna TJ, and Lamb FS. Cytokine activation of nuclear factor kappa B in vascular smooth muscle cells requires signaling endosomes containing Nox1 and ClC-3. *Circ Res* 101: 663–671, 2007.
36. Nagata D, Takeda R, Sata M, Satonaka H, Suzuki E, Nagano T, and Hirata Y. AMP-activated protein kinase inhibits angiotensin II-stimulated vascular smooth muscle cell proliferation. *Circulation* 110: 444–451, 2004.
37. Nass MM. Abnormal DNA patterns in animal mitochondria: ethidium bromide-induced breakdown of closed circular DNA and conditions leading to oligomer accumulation. *Proc Natl Acad Sci USA* 67: 1926–1933, 1970.
38. Passos JF, Saretzki G, Ahmed S, Nelson G, Richter T, Peters H, Wappler I, Birket MJ, Harold G, Schaeuble K, Birch–Machin MA, Kirkwood TB, and von Zglinicki T. Mitochondrial dysfunction accounts for the stochastic heterogeneity in telomere-dependent senescence. *PLoS Biol* 5: e110, 2007.
39. Pearlstein DP, Ali MH, Mungai PT, Hynes KL, Gewertz BL, and Schumacker PT. Role of mitochondrial oxidant generation in endothelial cell responses to hypoxia. *Arterioscler Thromb Vasc Biol* 22: 566–573, 2002.
40. Pedruzzi E, Guichard C, Ollivier V, Driss F, Fay M, Prunet C, Marie JC, Pouzet C, Samadi M, Elbim C, O'Dowd Y, Bens M, Vandewalle A, Gougerot–Pocidalo MA, Lizard G, and Ogier–Denis E. NAD(P)H oxidase Nox-4 mediates 7-ketocholesterol-induced endoplasmic reticulum stress and apoptosis in human aortic smooth muscle cells. *Mol Cell Biol* 24: 10703–10717, 2004.
41. Quijano C, Castro L, Peluffo G, Valez V, and Radi R. Enhanced mitochondrial superoxide in hyperglycemic endothelial cells: direct measurements and formation of hydrogen peroxide and peroxynitrite. *Am J Physiol Heart Circ Physiol* 293: H3404–H3414, 2007.
42. Robinson J and Cooper JM. Method of determining oxygen concentrations in biological media, suitable for calibration of the oxygen electrode. *Anal Biochem* 33: 390–399, 1970.
43. Szöcs K, Lassègue B, Sorescu D, Hilenski LL, Valppu L, Couse TL, Wilcox JN, Quinn MT, Lambeth JD, and Griendling KK. Upregulation of Nox-based NAD(P)H oxidases in restenosis after carotid injury. *Arterioscler Thromb Vasc Biol*. 22: 21–27, 2002.
44. Tahara EB, Barros MH, Oliveira GA, Netto LE, and Kowaltowski AJ. Dihydrolipoyl dehydrogenase as a source of reactive oxygen species inhibited by caloric restriction and involved in *Saccharomyces cerevisiae* aging. *FASEB J* 21: 274–283, 2007.
45. Tanaka S, Uehara T, and Nomura Y. Up-regulation of protein-disulfide isomerase in response to hypoxia/brain ischemia and its protective effect against apoptotic cell death. *J Biol Chem* 275: 10388–10393, 2000.
46. Terada LS. Specificity in reactive oxidant signaling: Think globally, act locally. *J Cell Biol* 174: 615–623, 2006.
47. Terada K, Manchikalapudi P, Noiva R, Jauregui HO, Stockert RJ, and Schilsky ML. Secretion, surface localization, turnover, and steady state expression of protein disulfide isomerase in rat hepatocytes. *J Biol Chem* 270: 20410–20416, 1995.
48. Touyz, RM, Yao, G, and Schiffrin, EL. c-Src induces phosphorylation and translocation of p47phox: Role in superoxide generation by angiotensin II in human vascular smooth muscle cells. *Arterioscler Thromb Vasc Biol* 23: 981–987, 2003.
49. Turrens JF. Mitochondrial formation of reactive oxygen species. *J Physiol* 552: 335–344, 2003.
50. Ushio–Fukai M. Localizing NADPH oxidase-derived ROS. *Sci STKE* 349: re8, 2006.
51. Yang Y, Song Y, and Loscalzo J. Regulation of the protein disulfide proteome by mitochondria in mammalian cells. *Proc Natl Acad Sci USA* 104: 10813–10817, 2007.
52. Yoshida T, Azuma H, Aihara K, Fujimura M, Akaike M, Mitsui T, and Matsumoto T. Vascular smooth muscle cell proliferation is dependent upon upregulation of mitochondrial transcription factor A (mtTFA) expression in injured rat carotid artery. *Atherosclerosis* 178: 39–47, 2005.
53. Wang W, Fang H, Groom L, Cheng A, Zhang W, Liu J, Wang X, Li K, Han P, Zheng M, Yin J, Wang W, Mattson MP, Kao JP, Lakatta EG, Sheu SS, Ouyang K, Chen J, Dirksen RT, and Cheng H. Superoxide flashes in single mitochondria. *Cell* 134: 279–290, 2008.

54. Wallace DC. Mitochondria as chi. *Genetics.* 179: 727–735, 2008.
55. Williams RS. Canaries in the coal mine: Mitochondrial DNA and vascular injury from reactive oxygen species. *Circ Res* 86: 915–916, 2000.
56. Zhao Q, Wang J, Levichkin IV, Stasinopoulos S, Ryan MT, and Hoogenraad NJ. A mitochondrial specific stress response in mammalian cells. *EMBO J* 21: 4411–4419, 2002.
57. Zylber E, Vesco C, and Penman S. Selective inhibition of the synthesis of mitochondria-associated RNA by ethidium bromide. *J Mol Biol* 44: 195–204, 1969.
58. Zylber E and Penman S. Mitochondrial-associated 4S RNA synthesis inhibition by ethidium bromide. *J Mol Biol* 46: 201–204, 1969.
59. Zorov DB, Juhaszova M, and Sollott SJ. Mitochondrial ROS-induced ROS release: An update and review. *Biochim Biophys Acta* 1757: 509–517, 2006.
60. Zou MH, Kirkpatrick SS, Davis BJ, Nelson JS, Wiles WG 4th, Schlattner U, Neumann D, Brownlee M, Freeman MB, and Goldman MH. Activation of the AMP-activated protein kinase by the anti-diabetic drug metformin *in vivo*. Role of mitochondrial reactive nitrogen species. *J Biol Chem* 279: 43940–43951, 2004.

Address reprint requests to:
Francisco R. M. Laurindo
Vascular Biology Laboratory
Heart Institute (InCor)
University of São Paulo School of Medicine
Av Eneas C Aguiar, 44 - Annex II, 9th floor
CEP 05403-000 São Paulo, Brazil

E-mail: expfrancisco@incor.usp.br

Date of first submission to ARS Central, December 3, 2008; date of acceptance, December 29, 2008.

This article has been cited by:

1. Timo Kahles , Ralf P. Brandes . Which NADPH Oxidase Isoform Is Relevant for Ischemic Stroke? The Case for Nox 2. *Antioxidants & Redox Signaling*, ahead of print. [Abstract] [Full Text HTML] [Full Text PDF] [Full Text PDF with Links]
2. Jannette Rodriguez-Pallares, Juan Andres Parga, Belen Joglar, Maria Jose Guerra, Jose Luis Labandeira-Garcia. 2012. Mitochondrial ATP-sensitive potassium channels enhance angiotensin-induced oxidative damage and dopaminergic neuron degeneration. Relevance for aging-associated susceptibility to Parkinson's disease. *AGE* **34**:4, 863-880. [CrossRef]
3. Eberhard Schulz , Philip Wenzel , Thomas Münzel , Andreas Daiber . Mitochondrial Redox Signaling: Interaction of Mitochondrial Reactive Oxygen Species with Other Sources of Oxidative Stress. *Antioxidants & Redox Signaling*, ahead of print. [Abstract] [Full Text HTML] [Full Text PDF] [Full Text PDF with Links]
4. Anthony J. Valente, Robert A. Clark, Jalahalli M. Siddesha, Ulrich Siebenlist, Bysani Chandrasekar. 2012. CIKS (Act1 or TRAF3IP2) mediates Angiotensin-II-induced Interleukin-18 expression, and Nox2-dependent cardiomyocyte hypertrophy. *Journal of Molecular and Cellular Cardiology* **53**:1, 113-124. [CrossRef]
5. Augusto C. Montezano, Rhian M. Touyz. 2012. Oxidative stress, Noxs, and hypertension: Experimental evidence and clinical controversies. *Annals of Medicine* **44**:S1, S2-S16. [CrossRef]
6. Dong-Hee Choi , Ana Clara Cristóvão , Subhrangshu Guhathakurta , Jongmin Lee , Tong H. Joh , M. Flint Beal , Yoon-Seong Kim . 2012. NADPH Oxidase 1-Mediated Oxidative Stress Leads to Dopamine Neuron Death in Parkinson's Disease. *Antioxidants & Redox Signaling* **16**:10, 1033-1045. [Abstract] [Full Text HTML] [Full Text PDF] [Full Text PDF with Links] [Supplemental material]
7. Ping Song, Ming-Hui Zou. 2012. Regulation of NAD(P)H oxidases by AMPK in cardiovascular systems. *Free Radical Biology and Medicine* **52**:9, 1607-1619. [CrossRef]
8. Francisco R.M. Laurindo, Luciana A. Pescatore, Denise de Castro Fernandes. 2012. Protein disulfide isomerase in redox cell signaling and homeostasis. *Free Radical Biology and Medicine* **52**:9, 1954-1969. [CrossRef]
9. Begoña Villar-Cheda, Antonio Dominguez-Meijide, Belen Joglar, Ana I. Rodriguez-Perez, Maria J. Guerra, Jose L. Labandeira-Garcia. 2012. Involvement of microglial RhoA/Rho-Kinase pathway activation in the dopaminergic neuron death. Role of angiotensin via angiotensin type 1 receptors. *Neurobiology of Disease* . [CrossRef]
10. Markus M. Bachschmid, Stefan Schildknecht, Reiko Matsui, Rebecca Zee, Dagmar Haeussler, Richard A. Cohen, David Pimental, Bernd van der Loo. 2012. Vascular aging: Chronic oxidative stress and impairment of redox signaling—consequences for vascular homeostasis and disease. *Annals of Medicine* 1-20. [CrossRef]
11. Michael E. Widlansky , David D. Gutterman . 2011. Regulation of Endothelial Function by Mitochondrial Reactive Oxygen Species. *Antioxidants & Redox Signaling* **15**:6, 1517-1530. [Abstract] [Full Text HTML] [Full Text PDF] [Full Text PDF with Links]
12. Sergey Dikalov. 2011. Cross talk between mitochondria and NADPH oxidases. *Free Radical Biology and Medicine* . [CrossRef]
13. Sergiy Sukhanov, Laura Semprun-Prieto, Tadashi Yoshida, A. Michael Tabony, Yusuke Higashi, Sarah Galvez, Patrice Delafontaine. 2011. Angiotensin II, Oxidative Stress and Skeletal Muscle Wasting. *The American Journal of the Medical Sciences* 1. [CrossRef]
14. Ali A Sovari, Marcelo G Bonini, Samuel C Dudley. 2011. Effective antioxidant therapy for the management of arrhythmia. *Expert Review of Cardiovascular Therapy* **9**:7, 797-800. [CrossRef]
15. Prakashsrinivasan Shanmugam, Anthony J. Valente, Sumanth D. Prabhu, Balachandar Venkatesan, Tadashi Yoshida, Patrice Delafontaine, Bysani Chandrasekar. 2011. Angiotensin-II type 1 receptor and NOX2 mediate TCF/LEF and CREB dependent WISP1 induction and cardiomyocyte hypertrophy. *Journal of Molecular and Cellular Cardiology* **50**:6, 928-938. [CrossRef]
16. A Silva, A Gírio, I Cebola, C I Santos, F Antunes, J T Barata. 2011. Intracellular reactive oxygen species are essential for PI3K/Akt/mTOR-dependent IL-7-mediated viability of T-cell acute lymphoblastic leukemia cells. *Leukemia* **25**:6, 960-967. [CrossRef]
17. Celio X.C. Santos, Narayana Anilkumar, Min Zhang, Alison C. Brewer, Ajay M. Shah. 2011. Redox signaling in cardiac myocytes. *Free Radical Biology and Medicine* **50**:7, 777-793. [CrossRef]
18. Shakil A. Khan , Jayasri Nanduri , Guoxiang Yuan , Brian Kinsman , Ganesh K. Kumar , Joy Joseph , Balaraman Kalyanaraman , Nanduri R. Prabhakar . 2011. NADPH Oxidase 2 Mediates Intermittent Hypoxia-Induced Mitochondrial Complex I Inhibition: Relevance to Blood Pressure Changes in Rats. *Antioxidants & Redox Signaling* **14**:4, 533-542. [Abstract] [Full Text HTML] [Full Text PDF] [Full Text PDF with Links]

19. Augusto C. Montezano, Dylan Burger, Graziela S. Ceravolo, Hiba Yusuf, Maria Montero, Rhian M. Touyz. 2011. Novel Nox homologues in the vasculature: focusing on Nox4 and Nox5. *Clinical Science* **120**:4, 131-141. [CrossRef]
20. Claudia Piccoli, Giovanni Quarato, Annamaria D'Aprile, Eustacchio Montemurno, Rosella Scrima, Maria Ripoli, Monica Gomaraschi, Pietro Cirillo, Domenico Boffoli, Laura Calabresi, Loreto Gesualdo, Nazzareno Capitanio. 2011. Native LDL-induced oxidative stress in human proximal tubular cells: multiple players involved. *Journal of Cellular and Molecular Medicine* **15**:2, 375-395. [CrossRef]
21. Dora Il'yasova, Kelly Kennedy, Ivan Spasojevic, Frances Wang, Adviye A. Tolun, Karel Base, Sarah P. Young, P. Kelly Marcom, Jeffrey Marks, David S. Millington, Mark W. Dewhirst. 2011. Individual responses to chemotherapy-induced oxidative stress. *Breast Cancer Research and Treatment* **125**:2, 583-589. [CrossRef]
22. Nynke E. Hahn, Christof Meischl, Paul J.M. Wijnker, Rene J.P. Musters, Maarten Fornerod, Hans W.R.M. Janssen, Walter J. Paulus, Albert C. van Rossum, Hans W.M. Niessen, Paul A.J. Krijnen. 2011. NOX2, p22^{phox} and p47^{phox} are Targeted to the Nuclear Pore Complex in Ischemic Cardiomyocytes Colocalizing with Local Reactive Oxygen Species. *Cellular Physiology and Biochemistry* **27**:5, 471-478. [CrossRef]
23. Rhian M Touyz, Ana M Briones. 2011. Reactive oxygen species and vascular biology: implications in human hypertension. *Hypertension Research* **34**:1, 5-14. [CrossRef]
24. Yang Wang, Shelley X.L. Zhang, David Gozal. 2010. Reactive oxygen species and the brain in sleep apnea#. *Respiratory Physiology & Neurobiology* **174**:3, 307-316. [CrossRef]
25. J.A. Parga, J. Rodríguez-Pallares, B. Joglar, C. Diaz-Ruiz, M.J. Guerra, J.L. Labandeira-Garcia. 2010. Effect of inhibitors of NADPH oxidase complex and mitochondrial ATP-sensitive potassium channels on generation of dopaminergic neurons from neurospheres of mesencephalic precursors. *Developmental Dynamics* **239**:12, 3247-3259. [CrossRef]
26. Andreas Daiber. 2010. Redox signaling (cross-talk) from and to mitochondria involves mitochondrial pores and reactive oxygen species. *Biochimica et Biophysica Acta (BBA) - Bioenergetics* **1797**:6-7, 897-906. [CrossRef]
27. Célio X.C. Santos , Leonardo Y. Tanaka , João Wosniak , Jr. , Francisco R.M. Laurindo . 2009. Mechanisms and Implications of Reactive Oxygen Species Generation During the Unfolded Protein Response: Roles of Endoplasmic Reticulum Oxidoreductases, Mitochondrial Electron Transport, and NADPH Oxidase. *Antioxidants & Redox Signaling* **11**:10, 2409-2427. [Abstract] [Full Text HTML] [Full Text PDF] [Full Text PDF with Links] [Supplemental material]
28. Alicia J. Kowaltowski, Nadja C. de Souza-Pinto, Roger F. Castilho, Anibal E. Vercesi. 2009. Mitochondria and reactive oxygen species. *Free Radical Biology and Medicine* **47**:4, 333-343. [CrossRef]
29. Halley Caixeta Oliveira, Elzira Elisabeth Saviani, Ione Salgado. 2009. NAD(P)H- and superoxide-dependent nitric oxide degradation by rat liver mitochondria. *FEBS Letters* **583**:13, 2276-2280. [CrossRef]